Andrusenko, I., Potticary, J. L., Hall, S. R., & Gemmi, M. (2020). A new olanzapine cocrystal obtained from volatile deep eutectic solvents and determined by 3D electron diffraction. *Acta Crystallographica Section B: Structural Science*, *76*(6), 1036-1044. https://doi.org/10.1107/S2052520620012779

A new olanzapine co-crystal obtained from volatile deep eutectic solvents and determined by 3D electron diffraction

Iryna Andrusenko,[a] Jason Potticary,[b] Simon R. Hall[b,*] and Mauro Gemmi[a,*]

*[a]Center for Nanotechnology Innovation@NEST, Istituto Italiano di Tecnologia, Piazza San Silvestro 12, Pisa Italy , [b]School of Chemistry, University of Bristol, Bristol, Cantock's Close, BS8 1TS, UK. *Correspondence e-mail: mauro.gemmi@iit.it; simon.hall@bristol.ac.uk*

Synopsis Identification and investigation of a new olanzapine phenol co-crystal.

Abstract A previously unknown co-crystal of olanzapine and phenol was identified from a volatile deep eutectic solvent as the intermediate species in the crystallization of olanzapine. This new nanocrystalline phase was investigated by electron diffraction, powder X-ray diffraction and differential scanning calorimetry. The structure was determined by simulated annealing using 3D electron diffraction data and confirmed using DFT-D optimizations. Olanzapine phenolate crystallizes in the triclinic space group $P\bar{1}$, supporting the hypothesis of a dimeric growth unit, where a centrosymmetric dimer is stabilized by multiple weak C–H···π interactions and forms double N–H···N hydrogen bonding with adjacent dimers.

Keywords: olanzapine; eutectic solvents; electron diffraction; crystal structure; centrosymmetric dimers.

1. Introduction

Olanzapine (2-methyl-4-(4-methyl-1-piperazinyl)-10*H*-thieno-[2,3-*b*][1,5]benzodiazepine) is an atypical antipsychotic drug that has proven efficacy against the positive and negative symptoms of schizophrenia, bipolar disorder and related psychoses (Fulton & Goa, 1997; Bhana *et al*., 2001). Olanzapine was first discovered while searching for a chemical analogue of clozapine that would not require haematological monitoring (Bitter *et al*., 2004). However, increasing experience with atypical antipsychotics in real-world clinical environments demonstrated that these drugs have a strong correlation with certain metabolic side effects, including weight gain, diabetes and dyslipidaemia (Rojo *et al*., 2015). Switching or combining different agents may be sufficient in some cases for reducing these undesired side effects, but in most instances, additional drug treatments are required. Therefore, the development of antipsychotic medications that offer the efficacy of olanzapine but reduce the associated risks could address a major unmet need in the treatment of different schizophreniform disorders (Citrome *et al*., 2019). Olanzapine phenolate represents a typical case of an intermediate product obtained during drug manufacturing. The detailed investigation of intermediate

phases allow for a better understanding of crystallization pathways and may play a prominent role in the future development of organic and inorganic (Andrusenko *et al*., 2011) chemistry.

Olanzapine is a molecule that crystallises with rich structural variety, having over 60 related structures reported in the Cambridge Structural Database. There are several olanzapine anhydrous polymorphic forms (Wawrzycka-Gorczyca *et al*., 2004; Thakuria & Nangia, 2011; Askin *et al*., 2019) as well as many hydrates (Capuano *et al*., 2003; Reutzel-Edens *et al*., 2003), solvates (Bojarska *et al*., 2013), co-crystals (Nanubolu & Ravikumar, 2017) and salts (Sarmah *et al*., 2016), obtained by diverse manufacturing processes. Additionally, computed crystal energy landscape screenings, have shown that other forms of olanzapine are possible (Bhardwaj *et al*., 2013).

Volatile deep eutectic solvents (VODES) have recently demonstrated their potential in reaching hard-to-access crystal polymorphs in other pharmaceutical systems (Andrusenko *et al*., 2019; Potticary *et al*., 2020), often under ambient conditions. In accordance with typical eutectic solvents, VODES are a mixture made of a hydrogen bond donor and an acceptor. However, unlike typical eutectic solvents, one of these co-formers is volatile and easily escapes the system, while the remaining, stable component forms a crystalline product. When a new polymorph is formed via VODES, it is common for the crystal size to be in the micro and nanometer range, making standard crystallographic investigations for structure solution a challenge.

The most efficient method for recognizing and understanding the intermolecular interactions that produce a given polymorph consists in the determination of its three-dimensional (3D) atomic structure. For crystals of 0.1 mm or larger, single crystal X-ray diffraction (XRD) is the method of choice, while for smaller crystals, powder XRD often appears as the only feasible option. However, powder XRD may fail due to accidental and systematic overlap of independent reflections even at medium resolution, which is emphasized if coherent crystalline areas are small or if the sample contains multiple phases. For poorly crystalline organic compounds, powder diffraction patterns often show only few intense peaks at low angles, while the diffraction intensity decays quickly, even at medium resolutions, eventually becoming part of the noise. Consequently, polymorphic modifications associated with nanocrystals are hard to identify. In these cases, 3D electron diffraction (3D ED) has proved to be a reliable method for the structure determination, even when only micrometric or sub-micrometric single crystals are available (Gemmi *et al*., 2019).

To fully exploit the potentialities of both powder XRD and 3D ED, we have adopted the following protocol: i) any new synthesis is first characterised by powder XRD; ii) if the pattern cannot be fully indexed with known structures, 3D ED data are collected from several crystals

to identify the phase (or phases) present in the sample and to measure the related unit cell(s); iii) if unknown phases are detected, their crystal structure are determined by 3D ED and refined by Rietveld refinement against powder XRD. This method was also used in case of olanzapine phenolate.

The olanzapine molecule consists of three fused rings (benzene, diazepine and thiophene) and one additional, satellite piperazine ring (Fig. 1). The boat conformation of the central 7-membered diazepine ring defines the overall shape of the molecule. The disparity between hydrogen bond donors to acceptors makes olanzapine highly amenable for the inclusion of solvents in the crystal lattice in order to balance hydrogen bonds (Infantes *et al*., 2007). Phenol is a simple molecule that has been widely explored and often used in eutectic systems for pharmaceutical applications. It can act as hydrogen bond donor and acceptor (Duarte *et al*., 2017).

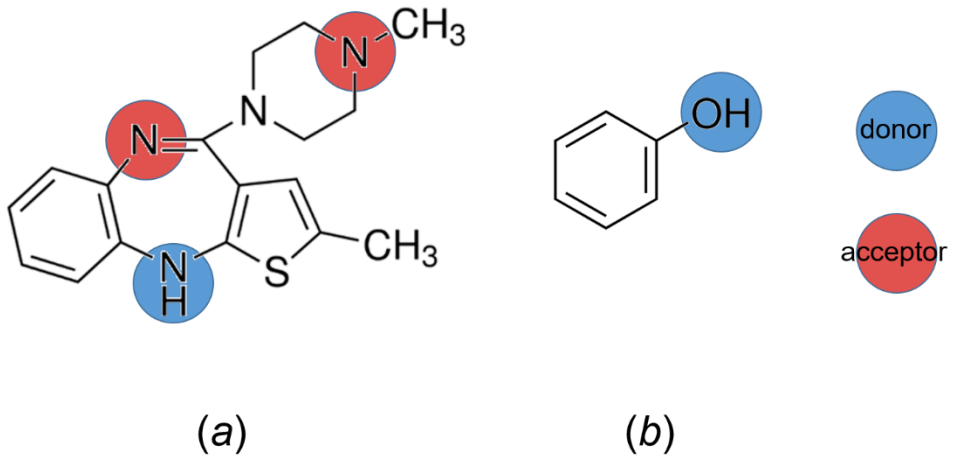

Figure 1 Molecular diagrams of (*a*) olanzapine and (*b*) phenol. Donor and acceptor groups are highlighted.

In the search for new olanzapine polymorphs by crystallization from VODES, we obtained a new intermediate crystalline complex of olanzapine and phenol. This phase appeared as submicrometric grains and therefore was structurally characterized by 3D ED.

2. Experimental

2.1. Crystallization

Olanzapine phenolate crystals were grown using the VODES method (Potticary *et al*., 2020). Solid olanzapine and phenol were mixed at a ratio of 1:8, respectively and left to spontaneously form a liquid at room temperature. This liquid was then dropped onto a glass surface and left to crystallize over 24 hours in a well-ventilated area, resulting in a white crystalline powder.

Initially, the crystallinity of the sample was ascertained using an optical microscope with cross-polarized filters.

2.2. Proton NMR

^{1}H-NMR analysis was conducted using a JEOL ECS 400 NMR spectrometer. Spectra were obtained from about 10 mg of sample dissolved in 1 mL of dimethyl sulfoxide-d_6 (Sigma-Aldrich, 99.5 %). All spectra were analysed using *MestReNova* software (version: 14.0.1-23559).

2.3. Thermal investigation

Melting points were recorded using differential scanning calorimetry (DSC) and was carried out using a TA Instruments Discovery DSC25. The cell was purged with N_2 gas at a rate of 50 mL·min^{-1}. Samples weighing between 2-10 mg were sealed in hermetic T_{zero} aluminum pans. Starting at 30 °C, samples were heated to temperatures at least 10 °C above observed endotherms. *TRIOS* software (version: 4.5.0.42498) was used for analysis of thermograms. Temperature and cell constant calibrations were carried out using a certified indium standard (verification: Temperature = 156.6 ± 0.5 °C, Enthalpy = 28.72 J·g^{-1} ± 4%).

2.4. Electron microscopy and 3D electron diffraction

Scanning electron microscopy (SEM) micrographs were taken on a JEOL IT300 using an accelerating voltage of 30 kV, samples were sputter coated with 15 nm of silver. High-angle annular dark-field scanning transmission electron microscopy (HAADF-STEM) imaging and electron diffraction (ED) data were recorded with a Zeiss Libra TEM operating at 120 kV and equipped with a LaB_6 source.

3D ED was performed in the same microscope in STEM mode after defocusing the beam in order to have a pseudo-parallel illumination on the sample, as described in Lanza *et al*. (2019). ED patterns were collected in Köhler parallel illumination with a beam size of about 150-200 nm in diameter, obtained using a 5 µm C2 condenser aperture. Data were recorded by a single-electron ASI MEDIPIX detector (Georgieva *et al.*, 2011). An extremely low dose illumination, corresponding to 0.01 el. Å^{-2} s^{-1}, was adopted in order to avoid beam damage. The total dose during data collection depends from many experimental parameters, like number of frames, exposure time and image tracking mode, and is therefore different for each data collection. A rough estimation of the total dose during a step-wise data collection is in the 1-5 el. Å^{-2} range, provided that the data are recorded with a single electron detector. With standard CCD the dose should be at least one order of magnitude higher.

The sample was gently crushed and directly loaded on a carbon-coated Cu TEM grid without any solvent or sonication. 3D ED acquisitions were performed when rotating the sample around

the TEM goniometer axis in steps of 1°, in total tilt ranges from 65° to 100°. Exposure time per frame was 1s. Camera length was 180 mm, allowing resolution in real space up to 0.7 Å. After each tilt, a diffraction pattern was acquired and the crystal position was tracked by STEM imaging (Gemmi & Lanza, 2019). During the experiment, the beam was precessed around the optical axis by an angle of 1°. Precession was obtained using a Nanomegas Digistar P1000 device. All data acquisitions were performed at room temperature.

3D ED data were analysed using the software *PETS* (Palatinus *et al*., 2019). Structure determination was obtained by simulated annealing (SA) as implemented in the software *SIR2014* (Burla *et al*., 2015). Resolution limit was set to 1.0 Å. SA is a stochastic algorithm that searches for the minimum of the cost function, gradually reducing the degrees of freedom (Kirkpatrick *et al*., 1983). This global optimization method works especially well for organic compounds, where the symmetry is generally low, no atoms are in special positions and there are strict geometrical constrains imposed by intra-molecular chemical bonding. For SA structure determination, the molecular model can be built considering the known chemical fragments or deduced from known polymorphic forms already reported in crystal structure databases. Each molecule can be modelled as a unique fragment, where atomic distances and coordination are known. This method was successfully applied to 3D ED data for the determination of covalent organic framework (Zhang *et al*., 2013) and important pharmaceuticals (Das *et al*., 2018). The olanzapine phenolate appears as an ideal case for SA because the olanzapine molecule has only one free torsion angle, while the phenol molecule is entirely rigid.

Data were treated with a fully kinematical approximation, assuming that I_{hkl} was proportional to $|F_{hkl}|^2$. The model determined by SA was refined with least-squares procedures embedded in the software *SHELXL* (Sheldrick, 2015). Geometrical ties were added stepwise to check the consistency of the model. All hydrogen atoms were generated in geometrically idealized positions.

2.5. Powder X-ray diffraction

Powder XRD data were acquired in Debye-Scherrer geometry using a STOE Stadi P equipped with Cu-$K_{\alpha 1}$ radiation (λ = 1.5406 Å), a Ge (111) Johansson monochromator from STOE & Cie and a MYTHEN2 1 K detector from Dectris. The sample was loaded in a borosilicate glass capillary (0.5 mm external diameter) and data were acquired in the range 5-50° 2θ with an interval of 0.003° between consecutive points. Data were processed with *GSAS-II* (Toby & Von Dreele, 2013).

2.6. Density functional theory optimization

Density functional theory (DFT) calculations were performed on *CRYSTAL17* (Dovesi *et al*., 2017) at the 6-31G level, using Perdew-Burke-Enzerhof (PBE0-d3) exchange correlation functional with semi-empirical dispersion corrections (DFT-D) to account for van der Waals interactions. Van der Waals radii were used as suggested by Federov *et al*. (2006). Both the space group and atomic coordinates obtained from the 3D ED were used as the input geometry.

3. Result and Discussion

3.1. Crystallization of a new co-crystal

Growth of olanzapine phenolate from a VODES resulted in a white powder with a needle diameter size between 5 - 30 µm (Fig. 2*a*). The powder is visible under cross-polarized light and undergoes extinction at 90° intervals, revealing an anisotropic, crystalline nature (Fig. 2*b*). SEM analysis shows that the needles are themselves layered (Fig. 2*c*) implying that an individual needle, if correctly isolated, would still be unsuitable for single crystal structure solution.

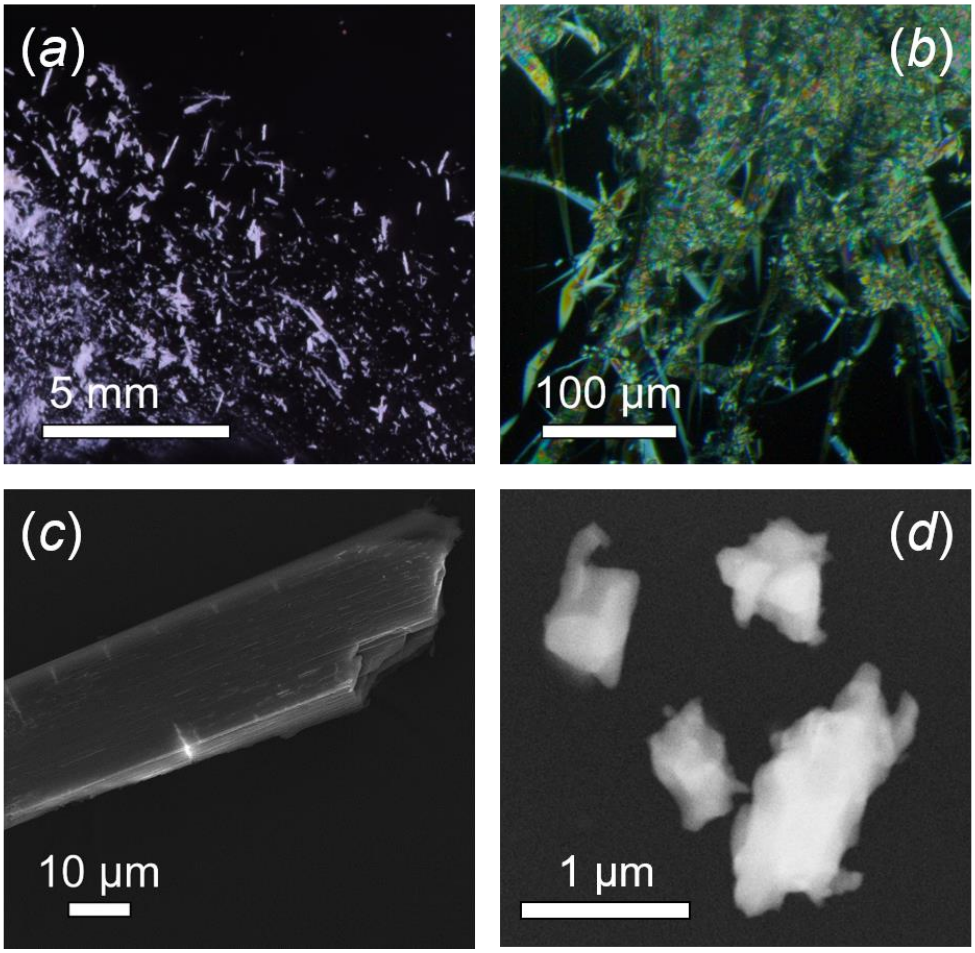

Figure 2 (*a*) Optical image of the white polycrystalline sample, (*b)* the same sample viewed through an optical microscope with cross-polarized filters (*c*) SEM micrograph of a typical crystal showing the

layered structure and (*d*) HAADF-STEM image of typical olanzapine phenolate crystals used for 3D ED data collections.

Analysis using ^{1}H-NMR shows a molar ratio of olanzapine to phenol of 1:1 phenol hydroxyl and thiophene protons integrating to 1.00 and 0.99, respectively (Fig. 3).

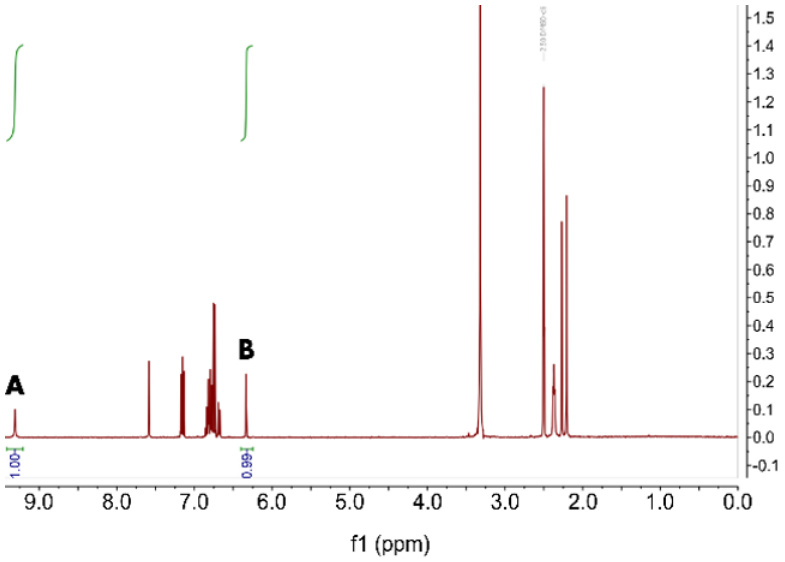

Figure 3 ^{1}H-NMR in DMSO-d_6 analysis showing the 1:1 ratio of the (A) phenol hydroxyl and (B) olanzapine single sp^2-bound thiophene proton.

Thermal analysis of the co-crystal (Fig. 4) shows a single melting point of 114.3 °C with no evidence of a phenol melt at the expected 40.5 °C. Unfortunately, due to the boiling point of phenol being 180.7 °C, temperatures at which olanzapine is expected to melt (195 °C) were not reached. This melt sits almost exactly between the melting points of the components (phenol and olanzapine melt at 40.5 and 195 °C, respectively). This linear trend in physical properties is not unexpected in a co-crystal of ratio 1:1, which distinguishes the structure from other disordered multi-component solids like typical solvates or clathrates.

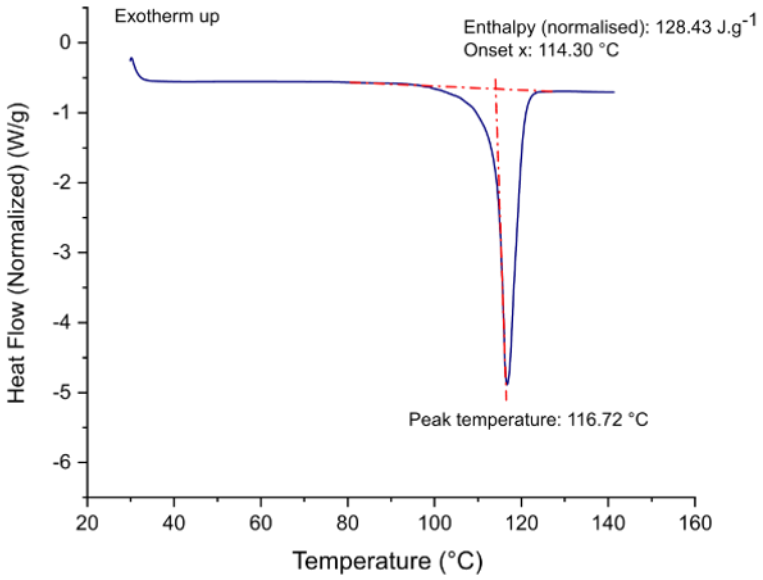

Figure 4 DSC thermogram of olanzapine phenolate.

3.2. 3D ED structure analysis

3D ED data were recorded from three crystal fragments with size less than 1 μm (Fig. 2*d*). Unfortunately, we cannot provide an accurate estimation of the crystal thickness. Taking into consideration that all observed crystals were not truly flat, their thickness was roughly estimated in about 50 nm. All 3D ED data sets were consistent with a triclinic cell with approximate parameters $a = 9.0$ Å, $b = 10.5$ Å, $c = 12.0$ Å, $\alpha = 95°$, $\beta = 95°$, $\gamma = 103°$ (Fig. 5). Cell parameters were refined and validated with a Pawley fitting against powder XRD data from which we obtained the refined lattice parameters: $a = 9.4051(9)$ Å, $b = 10.4236(11)$ Å, $c = 11.999619(8)$ Å, $\alpha = 96.686(4)°$, $\beta = 95.2878(27)°$, $\gamma = 104.474(3)°$. Taking into consideration the ratio between olanzapine and phenol (1:1), such a cell would conveniently host two pair of molecules ($Z = 2$). A close look at 3D ED reconstructions revealed no extinction features, pointing convincingly, to a triclinic space group: $P1$ (1) or $P\bar{1}$ (2).

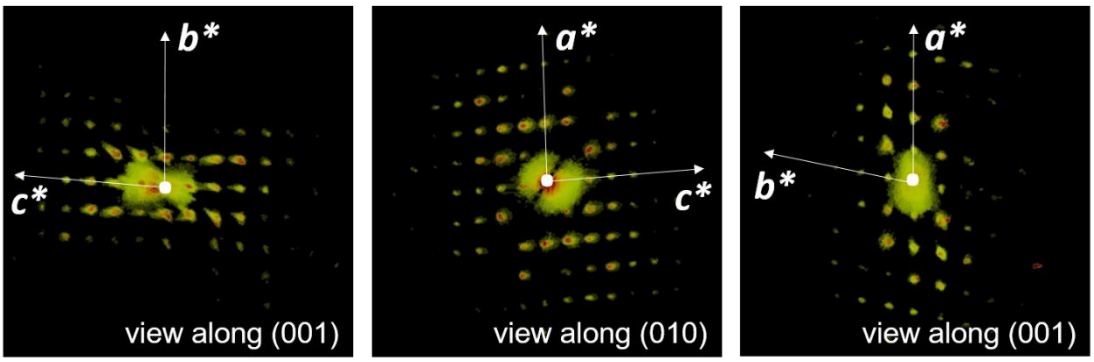

Figure 5 Reconstructions of 3D ED volume viewed along the main crystallographic directions.

Structure solution was performed by SA using the highest quality (the most complete with highest angular range and greatest resolution) 3D ED data set as an input. This global optimization method is the most frequently used, and the only one so far to applied to tomographic ED data (Zhang *et al*., 2013; Das *et al*., 2018). The two other data sets have lower quality, therefore the merging data was not applied in order to not reduce the quality of the merged intensities. To merge initially relatively poor 3D ED data makes sense only when taken alone each 3D ED data set misses a sufficient completeness for structure determination. Data completeness of 55% was enough for the obtaining a stable SA solution in a resolution range from 1.0 Å to 2.0 Å. This is also consistent with results reported by Das *et al*. (2018) for other organic structures. Therefore, we avoided to merge our three individual data sets in a unique one, which would be anyway affected by random noise introduced by the different contribution of dynamical effects related with the different dimension and shape of the crystals**.** After the SA runs, the best crystallo-chemical model in space group $P\bar{1}$ (2) was taken as an initial model for further refinements.

The structure of olanzapine phenolate was eventually, least-squares refined against 3D ED data imposing constraints on the aromatic ring and all hydrogen positions. Additionally, restraints for other interatomic distances and the planarity of the three major flat blocks that make up the molecules were imposed. More details about structure determination and refinement are reported in Table 1. The high values of agreement parameters can be explain by the relatively poorness of 3D ED data, not suitable for performing an *ab-initio* structure solution. Rietveld refinement, starting from the model obtained from the 3D ED data, converged to R_{wp} = 3.019%, R_F = 3.849%, R_{F2} = 3.512% without any significant modification (Fig. 6). The final structural model is shown in Fig .7.

The high difference between the measured value of the cell parameter *a* by 3D ED and the value refined by powder XRD can be explained by vacuum effect on phenol molecules that are oriented along [100] and partially evaporated upon heating under vacuum.

Table 1 Selected parameters from structure determination (*SIR2014*) and refinement (*SHELXL*) based on the 3D ED data.

Crystallographic information	
Asymmetric unit content	$C_{17}H_{20}N_4S{\cdot}C_6OH$
Z	2
Space group	$P\bar{1}$
a, Å	9.4051(9)
b, Å	10.4236(11)

c, Å	11.9619(8)
α, °	96.686(4)
β, °	95.2878(27)
γ, °	104.474(3)
Volume, Å^3	1118.75(5)
Structure solution	
Data resolution, Å	1.0
Sampled reflections, No.	2489
Independent reflections, No.	1271
Independent reflections coverage, %	55
Global thermal factor U_{iso}, Å^2	0.04053
R_{int} (F), %	17.81
CF, %	56.426
Structure refinement	
Data resolution, Å	1.0
R_{int} (F^2), %	15.11
Reflections (all), No.	1269
Reflections (> 4σ), No.	720
*R*1 (4σ), %	31.40
*R*1 (all), %	38.96
GooF	3.016

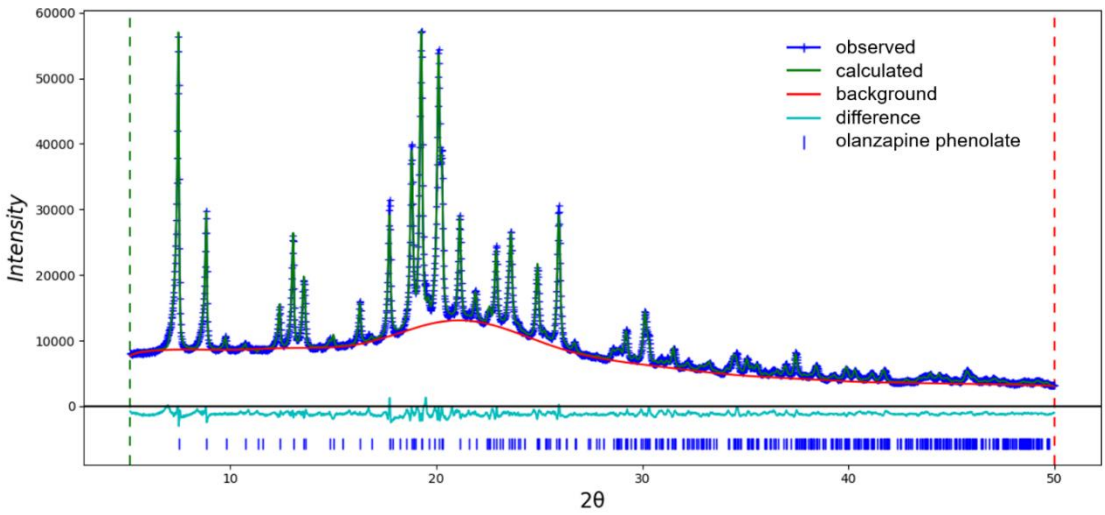

Figure 6 Final fit of 3D ED structural model against powder XRD data.

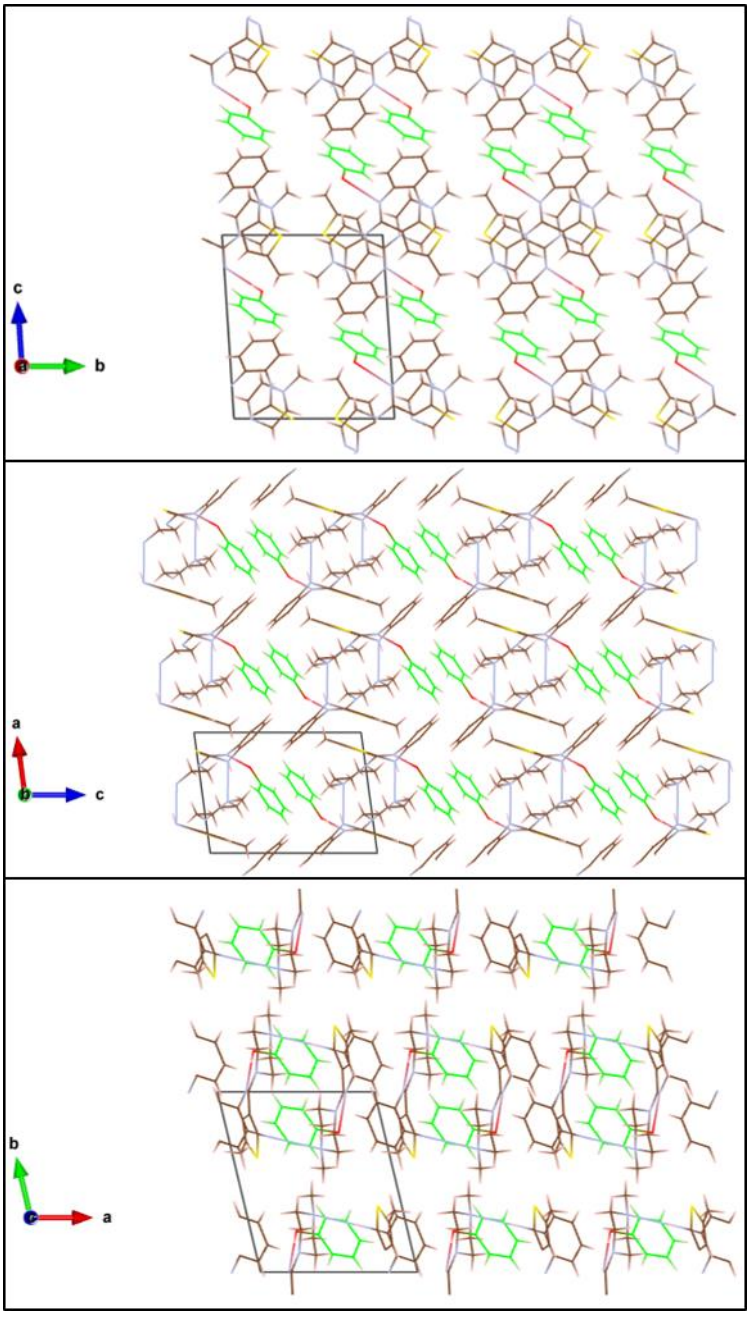

Figure 7 The final structural model of olanzapine phenolate. Phenol molecules are in green. N–H···O hydrogen bonds between olanzapine and phenol molecules are shown in red. Double hydrogen bonding (N–H···N) between two adjacent dimers, involving each olanzapine molecule in two N–H···N hydrogen bonds are shown in blue.

3.3. Optimization

DFT-D calculations correctly describe the structure with only minor structural differences expected of calculations done with zero thermal component. Comparison of the experimental and optimized structures show minor differences in the H-bond lengths, relative ring angle and phenol position but leave the overall structure intact indicative of a structural energy minima

(Fig. 8). Output details of DFT-D calculations are summarized in Table 2.

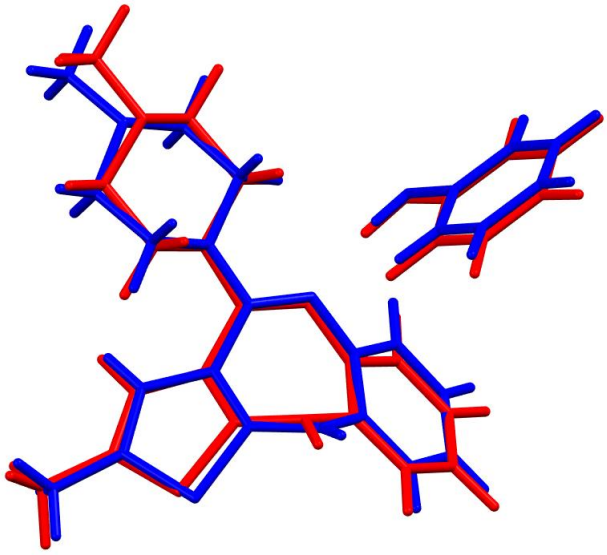

Figure 8 Overlay of powder XDR refined (blue) and optimized (red) structures of the olanzapine phenolate.

Table 2 Selected parameters from the experimental (3D ED), refined (powder XRD) and optimized (DFT-D) structures.

	3D ED experimental structure	Powder XRD refined structure	DFT-D optimized structure
Optimization steps, No.	–	-	98
N···O H-bond length, Å	2.891	2.695	2.734
N···N H-bond length, Å	3.241	4.224	2.962

3.4. Crystal packing and hydrogen bonding

In almost all known forms (anhydrous and hydrates), olanzapine adopts mirror-related conformations, which rapidly interconvert in solution by the inversion of the diazepine ring (Petcher & Weber, 1976). The two enantiomers are packed around the crystallographic inversion centres, compel olanzapine to crystallize in centrosymmetric space groups. Interestingly, no specific intermolecular interactions are needed to stabilize this dimer. According to Reutzel-Edens et al. (Reutzel-Edens *et al*., 2003), packing appears to be spatially driven, complementarity of the opposite enantiomers (electrostatic interaction). Conversely, other researchers (Wawrzycka-Gorczyca *et al*., 2004; Ravikumar *et al*., 2005; Thakuria &

Nangia, 2011) associated the pair stability with three types of multiple C–H···π contacts (Malone *et al*., 1997). Independently from the character of the intermolecular interactions, the centrosymmetric dimer observed in most of olanzapine crystal structures is generally considered the crystal building block from which different solid-state structures of olanzapine may assemble.

Ayala et al. (Ayala *et al*., 2006) showed that the intermolecular distances in olanzapine structures range from 4.665 Å to 5.120 Å. The shortest distance corresponds to the pure olanzapine polymorphs, while for hydrates the extra molecules placed among the centrosymmetric dimers expand their packing. Conversely, in olanzapine phenolate described in this paper, no expansion was observed and the intermolecular distance is comparable with the ones of the pure olanzapine polymorphs.

There are four known anhydrous forms of olanzapine. Three of them have been structurally resolved by XRD. The last, labelled as form III, has never been synthesized as pure phase and is only has associated with a theoretically predicted model (Askin *et al*., 2019). In anhydrous form I, (Wawrzycka-Gorczyca *et al*., 2004) dimers have a parallel packing (Fig. 9*a*), while in the anhydrous form II (Thakuria & Nangia, 2011) dimers have a herringbone arrangement (Fig. 9*b*). Both crystal structures are sustained by an N–H···N hydrogen bond.

The structural model of anhydrous form IV is the only one that does not contain dimer motifs. This structure was first predicted by energy minimization (Bhardwaj *et al*., 2013) and has been only recently crystallized and refined by Askin et al. (Askin *et al*., 2019). Here, single olanzapine molecules are ladder-like, packed by two N–H···N hydrogen bonds, which connect the diazepine N–H donor and the piperazine N acceptor (Fig. 9*c*).

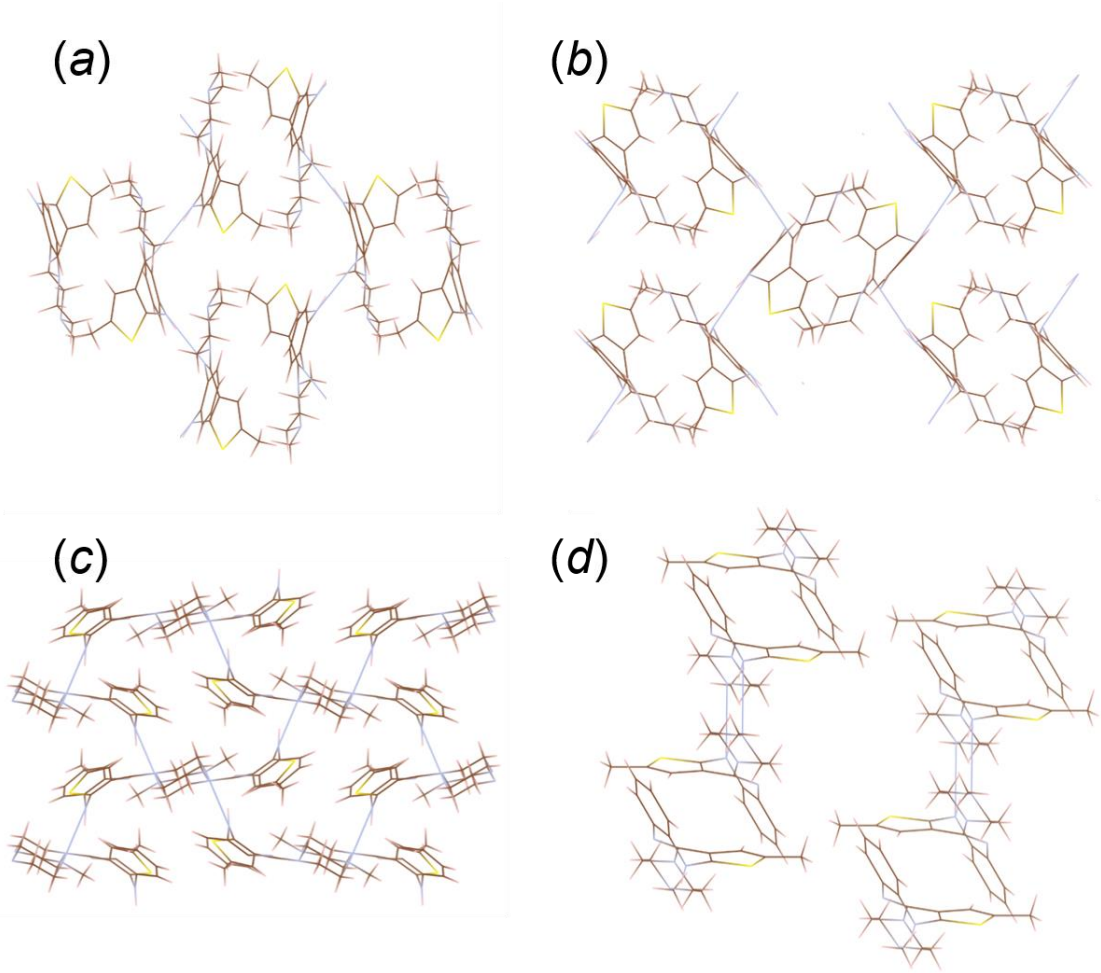

Figure 9 Comparison of molecular packing in different crystalline forms of olanzapine: (*a*) anhydrous form I, (*b*) anhydrous form II, (*c*) anhydrous form IV and (*d*) olanzapine phenolate (phenol molecule is not visualized). N–H···N hydrogen bonds between two adjacent dimers are sketched in blue.

The hydrogen bonding arrangements in hydrates are significantly different from that in pure crystal forms. By incorporating water into the crystal lattice, the donor-acceptor ratio becomes balanced, enabling both the acceptors on the olanzapine molecule to participate in hydrogen bonding. In all hydrated systems, the water molecules are held by two or three hydrogen bonding interactions (Reutzel-Edens *et al*., 2003).

The only reported "olanzapine-co-former" structure is olanzipinium nicotinate (Ravikumar *et al*., 2005). The coulombic interaction between olanzapine and nicotinic acid ions is supplemented by intermolecular N–H···O hydrogen bonds, forming catameric chains along the one main axis (Fig. 10*a*). Olanzapine dimers here are further stabilized by weak C–H···π interactions. No direct hydrogen bonding between dimers is present.

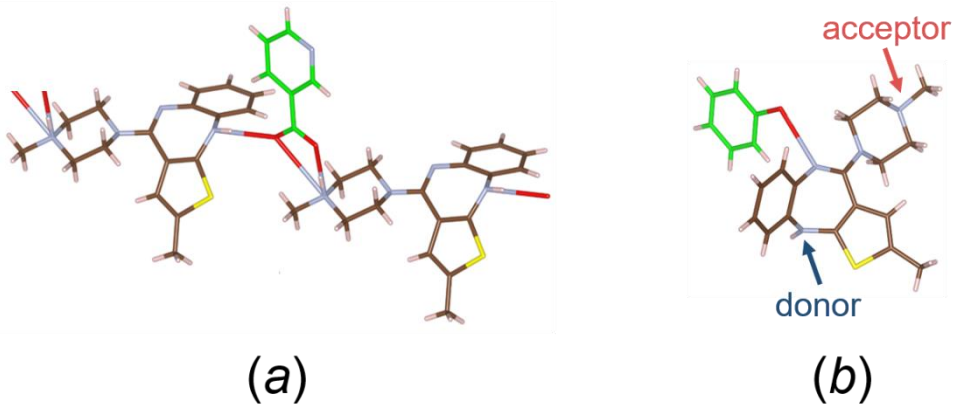

Figure 10 Comparison in molecular interaction between two "olanzapine-co-former" structures: (*a*) intermolecular N–H···O hydrogen bonds in olanzipinium nicotinate and (*b*) phenol compensation of one olanzapine acceptor in new olanzapine phenolate.

In the case of olanzapine phenolate, as in most of known olanzapine structures, the centrosymmetric dimers are present. Additionally, phenol acts as hydrogen bond donor for diazepine N, one of two potential olanzapine acceptors (Fig. 10*b*). In this way, phenol compensates for the disparity in the ratio of hydrogen bond donors-to-acceptors and allows for double hydrogen bonding (N–H···N) between two adjacent dimers. Consequently, interdimer connections are guaranteed by double N–H···N hydrogen bonds between two adjacent olanzapine molecules (Fig. 9*d*). Therefore, the structure consists of continuous dimeric chains stacked along [100]. Additionally, the presence of phenol appears to stabilize the structure in the other directions. Upon heating under vacuum for 7 days, the material assumes the characteristic yellow colour, adopting the structure of anhydrous olanzapine form I.

4. Conclusions

A new olanzapine phenolate was discovered as an intermediate product during the crystallization of olanzapine from volatile deep eutectic solvents. The ability of 3D ED to investigate nanocrystalline intermediate forms paves the way for a thorough understanding of crystallization pathways in pharmaceutical chemistry. Structure solution by single crystal XRD was not possible due to limited crystals sizes and morphologies, something pervasive throughout organic crystallization. Nevertheless, the structure was solved from electron diffraction data collected from single nanocrystal using the 3D ED approach. The stability of the result was confirmed by DFT-D structural optimization and the molecular ratio of the co-crystal confirmed via NMR. The dimeric packing of olanzapine phenolate resembles the one observed in the three known anhydrous olanzapine polymorphs and differs from hydrated and other co-crystallized forms. Complete information about the intermediate structure of co-crystals during the formation process is essential for discovery of possible new polymorphs,

not just of olanzapine but in any organic system.

Accession Codes

CCDC 2027602 contains the supplementary crystallographic 3D ED data for this paper.

CCDC 2030951 contains the supplementary crystallographic powder XRD data for this paper.

These data can be obtained free of charge via www.ccdc.cam.ac.uk/data_request/cif, or by emailing data_request@ccdc.cam.ac.uk, or by contacting The Cambridge crystallographic Data Centre, 12 Union Road, Cambridge CB2 1EZ, UK; fax: +44 1223 336033.

Acknowledgements The authors would like to thank Dr Sean Davis for obtaining the SEM images; Dr Arianna E. Lanza and Dr Enrico Mugnaioli for assistance and helpful discussions regarding the refinement of the final structure. S.R.H. and J.P. acknowledge MagnaPharm a collaborative research project funded by the European Union's Horizon 2020 Research and Innovation programme (grant No.736899). I.A and M.G. acknowledge the Regione Toscana for funding the purchase of the Timepix through the FELIX project (POR CREO FERS 2014-2020).

References

[Andrusenko, I., Mugnaioli, E., Gorelik, T. E., Koll, D., Panthöfer, M., Tremel, W. & Kolb, U. (2011). *Acta Cryst.* B**67**, 218-225.]

[Andrusenko, I., Hamilton, V., Mugnaioli, E., Lanza, A, Hall, C., Potticary, J., Hall, S. R. & Gemmi, M. (2019). *Angew. Chem. Int. Edit.* **131**, 11035.]

[Askin, S., Cockcroft, J. K., Price, L. S., Gonçalves, A. D., Zhao, M., Tocher, D. A., Williams, G. R., Gaisford, S. & Craig, D. Q. M. (2019). *Cryst. Growth Des.* **19**, 2751-2757.]

[Ayala, A. P., Siesler, H. W., Boese, R., Hoffmann, G. G., Polla, G. I. & Vega, D. R. (2006). *Int. J. Pharm.* **326**, 69-79.]

[Bhana, N., Forset, R. H., Olney, R. & Plosker, G. L. (2001). *Drugs* **61**, 111-161.]

[Bhardwaj, R. M., Price, L. S., Price, S. L., Reutzel-Edens, S. M., Miller, G. J., Oswald, I. D. H., Johnston, B. F. & Florence, A. J. (2013). *Gryst. Growth Des.* **16**, 1047-1055.]

[Bitter, I., Dossenbach, M. R. K., Brook, S., Feldman, P. D., Metcalfe, S., Gagiano, C. A., Furedi, J., Bartko, G., Janka, Z., Banki, C. M., Kovacs, G. & Breier, A. (2004). *Prog. Neuro-Psychopharmacol. Biol. Psychiatry* **28**, 173-180.]

[Bojarska, J., Maniukiewicz, W. & Sieroń, L. (2013). *Acta Cryst.* E**69**, 781-786.]

[Burla, M. C., Caliandro, R., Carrozzini, B., Cascarano, G. L., Cuocci, C., Giacovazzo, C., Mallamo, M., Mazzone, A. & Polidori, G. (2015). *J. Appl. Cryst.* **48**, 306-309.]

[Capuano, B., Crosby, I. T., Fallon, G. D., Lloyd, E. J., Yuriev, E. & Egan, S. J. (2003). *Acta Cryst.* E**59**, 01367-01369.]

[Citrome, L., McEvoy, J. P., Todtenkopf, M. S., McDonnell, D. & Weiden, P. J. (2019). *Neuropsychiatr. Dis. Treat.* **15**, 2559-2569.]

[Das, P. P., Mugnaioli, E., Nicolopoulos, S., Tossi, C., Gemmi, M., Galanis, A., Borodi, G. & Pop, M. M. (2018). *Org. Process Res. Dev.* **22**, 1365–1372.]
[Duarte, A. R. C., Ferreira, A. S. D., Barreiros, S., Cabrita, E., Reis, R. L. & Paiva, A. (2017). *Eur. J. Pharm. Biopharm.* **114**, 296-304.]
[Fulton, B. & Goa, K. L. (1997). *Drugs* **53**, 281-298.]
[Gemmi, M. & Lanza, A. (2019). *Acta Cryst.* B**75**, 495-504.]
[Gemmi, M., Mugnaioli, E., Gorelik, T. E., Kolb, U., Palatinus, L., Boullay, F.,Hovmöller, S. & Abrahams, J. P. (2019). *ACS Cent. Sci.* **5**, 1315-1329.]
[Georgieva, D. Jansen, J., Sikharulidze, I., Jiang, L., Zandbergen, H. W. & Abrahams, J. P. (2011). *J. Instrum.* **6**, C01033.]
[Infantes, L., Fábián, L. & Motherwell, W. D. S. (2007). *CrystEngComm* **9**, 65-71.]
[Kirkpatrick, S., Gelatt Jr., C. D. & Vecchi, M. P. (1983). *Science*, **220**, 671-680.]
[Lanza, A., Margheritis, E., Mugnaioli, E., Cappello, V., Garau, G. & Gemmi, M. (2019). *IUCrJ* **6**, 178-188.]
[Nanubolu, J. B. & Ravikumar, K. (2017). *CrystEngComm* **19**, 355-366.]
[Palatinus, L. Brázda, P., Jelínek, M., Hrdá, J., Steciuk, G. & Klementová, M. (2019). *Acta Cryst.* B**75**, 512-522.]
[Petcher, T. J. & Weber, H.-P. (1976). *J. Chem. Soc., Perkin Trans. II*, 1415-1420.]
[Potticary, J., Hall, C., Hamilton, V., McCabe, J. F. & Hall, S. R. (2020). *Cryst. Growth Des.* **20**, 2877-2884.]
[Ravikumar, R., Swamy, G. Y. S. K., Sridhar, B. & Roopa, S. (2005). *Acta Cryst.* E**61**, 02720-02723.]
[Reutzel-Edens, S. M., Bush, J. K., Magee, P. A., Stephenson, G. A. & Byrn, S. R. (2003). *Cryst. Growth Des.* **3**, 898-907.]
[Rojo, L. E., Gaspar, P. A., Silva, H., Risco, L., Arena, P., Cubillos-Robles, K. & Jara, B. (2015). *Pharmacol Res.* **101**, 74-85.]
[Sarmah, K. K., Sarma, A., Roy, K., Rao, D. R. & Thakuria, R. (2016). *Cryst. Growth Des.* **16**, 1047-1055.]
[Sheldrick, G. M. (2015). *Acta Cryst.* C**71**, 3-18.]
[Thakuria, R. & Nangia, A. (2011). *Acta Cryst.* C**67**, 0461-0463.]
[Toby, B. H. & Von Dreele, R. B. (2013). *J. Appl. Cryst.* **46**, 544-549.]
[Wawrzycka-Gorczyca, I., Koziol, A. E., Glice, M. & Cybulski, J. (2004). *Acta Cryst.* E**60**, 066-068.]
[Zhang, Y.-B., Su, J., Furukawa, H., Yun, Y., Gándara, F., Doung, A., Zou, X. & Yaghi, O. M. (2013). *J. Am. Chem. Soc.* **135**, 16336-16339.]